

Communication

## The Composites of Cationic Polyelectrolyte and Glutathione-capped Quantum Dots for Selective Fluorescence Detection of $\text{Cu}^{2+}$

Fang-Chen Liu, Chien-Chih Shen and Wei-Lung Tseng\*

*Department of Chemistry, National Sun Yat-sen University, Taiwan, R.O.C.*

Received January 10, 2011; Accepted April 7, 2011; Published Online April 22, 2011

A new composite of poly(diallyldimethylammonium chloride) (PDDAC) and glutathione-capped ZnHgSe quantum dots (GSH-QDs) has been developed for sensing  $\text{Cu}^{2+}$  in aqueous solution on the basis of fluorescence quenching. The formation of the composite is dominated through the electrostatic interaction between cationic PDDAC and anionic GSH-QDs. When  $\text{Cu}^{2+}$  collides with PDDA/GSH-QDs composites,  $\text{Cu}^{2+}$  displaces the Zn and/or Hg in the ZnHgSe QDs and forms extremely low soluble particles of CuSe onto the surface of QDs. As a result, the fluorescence intensity of QDs is quenched efficiently. Compared to GSH-QDs, PDDA/GSH-QDs composites exhibited better selectivity toward  $\text{Cu}^{2+}$  as a result of minimizing the electrostatic interaction between metal ions and the ligands. The selectivity of PDDA/GSH-QDs composites toward  $\text{Cu}^{2+}$  was further improved by increasing glycine concentration and optimizing the pH of the solution. Under the optimal conditions, PDDA/GSH-QDs composites provided the limits of detection for  $\text{Cu}^{2+}$  at a signal-to-noise ratio of 3 of 0.2 nM ( $\sim 2.0$  ppt). We believe that this probe has great potential for the detection of  $\text{Cu}^{2+}$  in environmental waters.

**Keywords:** Quantum dots; Glutathione; Poly(diallyldimethylammonium chloride); Fluorescence quenching.

### INTRODUCTION

The quantification of heavy metal ions in the aquatic environment and biological system is of considerable interest because they pose severe risks for human health.<sup>1</sup> Copper is one of the heavy metals and widely used for industries and agriculture, resulting in the pollution of the surrounding environment such as surface water and groundwater.<sup>2</sup> Although copper is an essential trace element for human growth and development,<sup>3</sup> exposure to high level of  $\text{Cu}^{2+}$  can cause gastrointestinal disturbance and liver damage.<sup>4</sup> Besides, the concentration of  $\text{Cu}^{2+}$  in human body reflect numerous, serious human afflictions such as Menkes and Wilson diseases,<sup>5</sup> Alzheimer's disease,<sup>6</sup> amyotrophic lateral sclerosis,<sup>7</sup> and prion diseases.<sup>8</sup> The maximum level of copper in drinking water permitted by the United States Environmental Protection Agency is 1.3 ppm ( $\sim 20$   $\mu\text{M}$ ).<sup>9</sup> Owing to the environmental and clinical significance of  $\text{Cu}^{2+}$ , the detection of  $\text{Cu}^{2+}$  continues to be of interest.

The most common approaches of detection of  $\text{Cu}^{2+}$  are atomic absorption spectroscopy<sup>10</sup> and inductively coupled plasma mass spectrometry (ICP-MS).<sup>11</sup> However, these instrument techniques are rather complicated, time-consuming, and high-cost, as well as not suitable for point-of-use applications. High selective and sensitive detection of  $\text{Cu}^{2+}$  have been also performed by modification of suitable ligands on the surface of electrodes.<sup>12,13</sup> For example, a gold electrode modified with cysteine has been demonstrated to be useful for sensing  $\text{Cu}^{2+}$ .<sup>12</sup> Fluorescence quenching based on the formation of  $\text{Cu}^{2+}$ -ligand complexes is an alternative approach for simple and rapid detection of  $\text{Cu}^{2+}$  in an aqueous solution.<sup>14-16</sup> In general, the fluorescent sensor consisted of a fluorophore and a complexing unit linked together through an appropriate spacer. Besides, fluorescence resonance energy transfer from the fluorophore to the quencher has been applied to sensing of  $\text{Cu}^{2+}$  with high sensitivity and selectivity.<sup>17-19</sup>

Recently, colloidal semiconductor nanocrystals (quan-

Special issue for the nanotechnology-related analytical chemistry

\* Corresponding author. E-mail: Tel: 07-5252000 ext. 3925; Fax: 011-886-7-3684046; E-mail: tsengwl@mail.nsysu.edu.tw

tum dots, QDs) such as CdSe, CdS, and CdTe, have also been considered as a  $\text{Cu}^{2+}$  sensor on the basis of fluorescence quenching.<sup>20-25</sup> A variety of capping agents is used to improve the selectivity of QDs toward  $\text{Cu}^{2+}$ . Bovine serum albumin and histidine-containing peptide, which have high affinity with  $\text{Cu}^{2+}$ , have been used to decorate the CdSe-ZnS and CdS QDs, respectively.<sup>20,21</sup> Thioglycerol-capped CdS QDs have been demonstrated to be sensitive to  $\text{Cu}^{2+}$  and  $\text{Fe}^{3+}$ .<sup>22</sup> The same phenomenon has been discovered in the case of 2-mercaptoethane sulfonic acid-modified CdSe QDs.<sup>23</sup> The addition of  $\text{F}^-$  to a solution of QDs can further improve the selectivity of QDs owing to the formation of the colorless complex  $\text{FeF}_6^{3-}$ . Selective fluorescence quenching of 3-mercaptopropionic acid-capped CdTe QDs has been carried out in the presence of  $\text{Cu}^{2+}$  while a solution contains masking agents for  $\text{Al}^{3+}$  and  $\text{Hg}^{2+}$ .<sup>24</sup> A bright-orange CdTe nanowires, which were made through self-assembly thioglycolic acid-capped CdTe QDs, have been utilized for selective detection of  $\text{Cu}^{2+}$ .<sup>25</sup> Although these above mentioned approaches all provide high sensitivity for detection of  $\text{Cu}^{2+}$ , the solution of problems associated with cross-sensitivity toward other metal ions, limitation in practical use, short dynamic range, and additional masking agents remains a challenge.

Herein, we report a highly selective and selective approach to sense  $\text{Cu}^{2+}$  by means of the composites of cationic polyelectrolyte and glutathione-capped QDs (GSH-QDs). The QD-based sensor was constructed by blending cationic poly(diallyldimethylammonium chloride) (PDDAC) with the opposite charge of GSH-QDs. Note that ZnHgSe QDs modified with GSH offer the advantages of high quantum yields, low toxicity, easy preparation, and high photostability.<sup>26</sup> As compared to GSH-QDs, PDDA/GSH-QDs composites provide better selectivity toward  $\text{Cu}^{2+}$ , but at the expense of sensitivity. Under optimum buffer and pH conditions, the selectivity of this probe for  $\text{Cu}^{2+}$  is remarkably high over other metal ions and the lowest detectable concentration of  $\text{Cu}^{2+}$  is 0.6 nM ( $\sim 3.8$  ppt).

## RESULTS AND DISCUSSION

### Mechanism of Fluorescence Quenching of GSH-QDs and PDDA/GSH-QDs Composites

According to the previous studies, it is proposed that  $\text{Cu}^{2+}$ -induced fluorescence quenching of GSH-capped ZnHgSe QDs can be illustrated through two possible mechanisms: First, because of strong coordination of  $\text{Cu}^{2+}$  to the

carboxyl group of GSH, the effective electron transfer from GSH to  $\text{Cu}^{2+}$  occurs onto the surface of QDs and results in the reduction of  $\text{Cu}^{2+}$  to  $\text{Cu}^+$ .<sup>29</sup> The formation of  $\text{Cu}^+$  induces the effective quenching of the fluorescence of QDs through facilitating nonradiative recombination of excited electron in the conduction band and holes in the valence band. On the other hand,  $\text{Cu}^{2+}$  displaces the Zn and/or Hg in the ZnHgSe QDs, leading to forming extremely low soluble particles of CuSe onto the surface of QDs.<sup>30</sup>

Once the CuSe particles deposits onto the surface of QDs, the fluorescence intensity of QDs is quenched efficiently. This phenomenon is attributed to that the fluorescence intensity of QDs is extremely susceptible to their surface states. Through two possible mechanisms, Fig. 1A displays that the addition of 10 M  $\text{CuCl}_2$  to a solution of GSH-QDs, which was prepared in 100 mM glycine at pH 7.0, resulted in a ca. 270-fold decrease in fluorescence. Under identical buffer conditions, fluorescence quenching of PDDA/GSH-QDs composites was observed upon the addition of 10  $\mu\text{M}$   $\text{CuCl}_2$  (Fig. 1B). However, the quenching efficiency of the composites was lower than that of GSH-QDs. The result suggested that the use of PDDA as capping agents can block the coordination of  $\text{Cu}^{2+}$  to the carboxyl group of GSH because of the electrostatic repulsion between PDDA and  $\text{Cu}^{2+}$ . Thus, the fluorescence quenching of QDs merely occurs when  $\text{Cu}^{2+}$  collides with PDDA/GSH-QDs composites. This collision provides the opportunity for  $\text{Cu}^{2+}$  to pass through the PDDA layer and then form CuSe particles onto the surface of QDs. The similar results were obtained in the case of analysis of other copper salts, such as  $\text{Cu}(\text{ClO}_4)_2$  and  $\text{CuSO}_4$  (data not shown); the result implied that the counter anions exert a negligible effect on our probe. Moreover, after GSH-QDs were modified with cationic PDDA, a small decrease in fluorescence intensity was discovered. Except for this slight disadvantage, we did not observe any difference in the fluorescence spectrum between GSH-QDs and PDDA/GSH-QDs composites.

Next, the formation of PDDA/GSH-QDs composites was demonstrated by DLS and DFM. Fig. 2A shows that the particle size of PDDA/GSH-QDs composites, which was measured by DLS, is approximately 12-fold larger than that of GSH-QDs. The result indicated that the PDDA molecules have been successfully attached to GSH-QDs. Moreover, we obtained the nano-size PDDA-QD particle composites, rather than micro-size particle. This feature can assist the probe in rapidly sensing the target analyte be-

cause they possess higher surface area-to-volume ratios. Fig. 2B displays dark-field scattering images of GSH-QDs and PDDA/GSH-QDs composites, respectively. In contrast to the scattering images of GSH-QDs, the bright spots were discovered in the case of PDDA/GSH-QDs composites. Because of the low scattering intensity and faster diffusion of 4.5-nm QDs, the scattering light of GSH-QDs was hardly observed by DFM. These results provided clear evidences for the formation of PDDA/GSH-QDs composites, which appropriately contain 5.0-40.0 particles per the composite.

### Selectivity of PDDA/GSH-QDs Composites

We also investigated the changes in the fluorescence

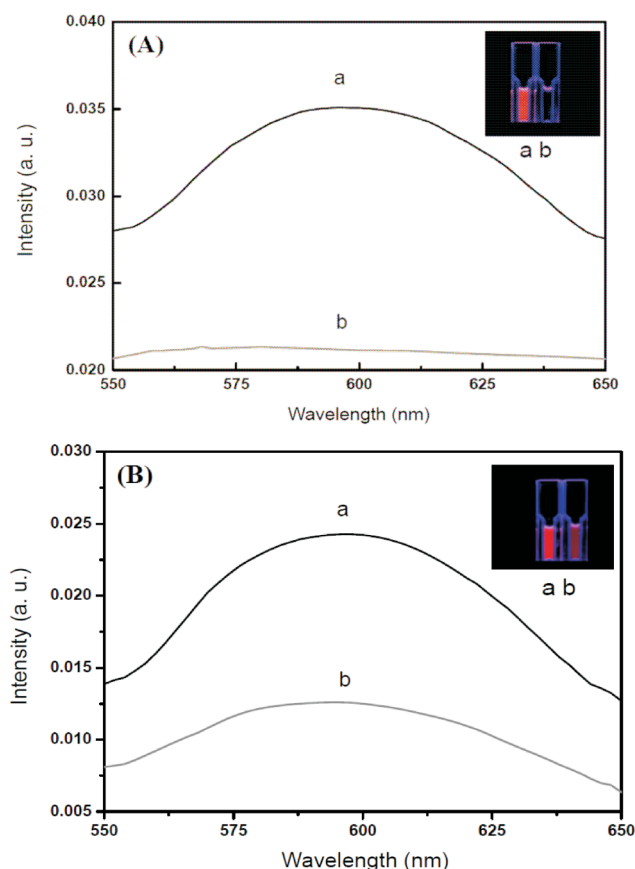


Fig. 1. The fluorescent spectra of (A) GSH-QDs and (B) PDDA/GSH-QDs composites in the (a) absence and (b) presence of  $10\ \mu\text{M}\ \text{Cu}^{2+}$ . Buffer: 100 mM glycine at pH 7.0. The incubation time is 40 min. The excitation wavelength was set at 488 nm. The fluorescence intensities ( $I$ ) are plotted in arbitrary units (au). Inset: Photograph of a solution of (a) QDs and (b) QDs and  $10\ \mu\text{M}\ \text{Cu}^{2+}$  under 365-nm UV light.

spectra of GSH-QDs and PDDA/GSH-QDs composites that occurred within 40 min of separately adding the following metal ions ( $10\ \mu\text{M}$ ):  $\text{Li}^+$ ,  $\text{Na}^+$ ,  $\text{K}^+$ ,  $\text{Ca}^{2+}$ ,  $\text{Ba}^{2+}$ ,  $\text{Mn}^{2+}$ ,  $\text{Fe}^{2+}$ ,  $\text{Fe}^{3+}$ ,  $\text{Co}^{2+}$ ,  $\text{Ni}^{2+}$ ,  $\text{Cu}^{2+}$ ,  $\text{Zn}^{2+}$ ,  $\text{Cd}^{2+}$ ,  $\text{Hg}^{2+}$ , and  $\text{Pb}^{2+}$ . Two kinds of QD-based nanomaterials were prepared in 100 mM glycine at pH 7.0. Fig. 3A shows that the addition of  $\text{Na}^+$ ,  $\text{K}^+$ ,  $\text{Ca}^{2+}$ ,  $\text{Ba}^{2+}$ ,  $\text{Fe}^{2+}$ ,  $\text{Fe}^{3+}$ ,  $\text{Co}^{2+}$ ,  $\text{Cd}^{2+}$ , and  $\text{Pb}^{2+}$  to a solution of GSH-QDs led to an increase in the ratio of fluorescence intensity ( $I_0/I$ ), whereas the remaining ions exhibited no significant effects under identical conditions. Note that  $I_0$  and  $I$  are the fluorescence intensity of GSH-QDs in the absence and presence of metal ions, respectively. The results indicated that the selectivity of GSH-QDs toward  $\text{Cu}^{2+}$  is rather poor. More importantly, the fluorescence intensity of GSH-QDs is very sensitive to  $\text{Na}^+$  and  $\text{K}^+$ , which are abundant in urine and seawater samples.<sup>31</sup> The fluorescence of GSH-QDs quenched by alkaline ions is probably due to the electrostatic interaction between the carboxyl group of GSH and alkaline ions. Thus, it is suggested that GSH-QDs is not appropriate for the analysis of  $\text{Cu}^{2+}$  in high-salt matrix. In contrast to the former probe, Fig. 3B

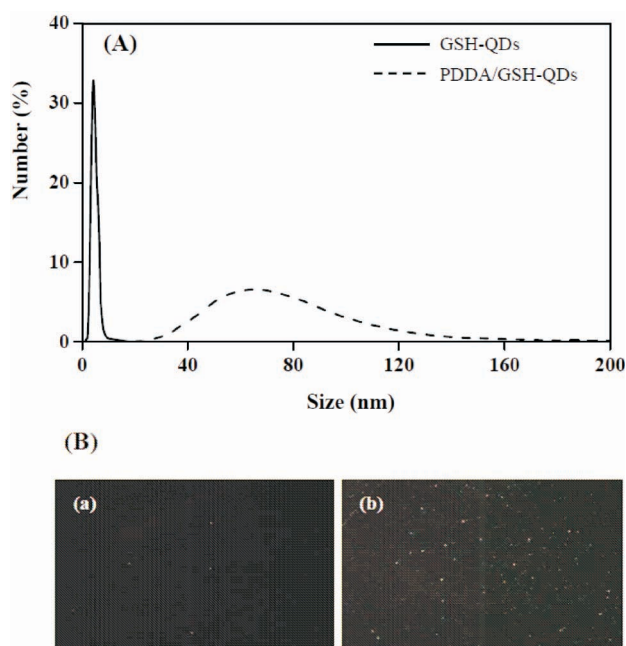


Fig. 2. (A) The particle sizes of GSH-QDs and PDDA/GSH-QDs composites were obtained by DLS measurement. (B) Dark-field scattering images of (a) GSH-QDs and (b) PDDA/GSH-QDs composites. Exposure times: XX ms; scattering detection area using a  $50\times$  objective:  $755\ \mu\text{m} \times 545\ \mu\text{m}$ , which corresponds to  $4080$  (horizontal)  $\times 3074$  (vertical) pixels.

displays that PDDA/GSH-QDs composites were capable of avoiding the interferences of  $\text{Na}^+$ ,  $\text{K}^+$ ,  $\text{Ca}^{2+}$ ,  $\text{Ba}^{2+}$ , and  $\text{Cd}^{2+}$ . The results indicated that PDDA molecules play a vital role in minimizing the electrostatic interaction between metal ions and the ligands. However, the interferences of  $\text{Fe}^{2+}$ ,  $\text{Fe}^{3+}$ ,  $\text{Co}^{2+}$ , and  $\text{Pb}^{2+}$  were still present when PDDA/GSH-QDs composites was used to sense  $\text{Cu}^{2+}$ . Fortunately, specificity of PDDA/GSH-QDs composites toward  $\text{Cu}^{2+}$ , with respect to the other metal ions, was readily achieved by increasing the concentration of glycine to 800 mM (Fig. 4A). The role of glycine in bulk solution is a masking agent that forms stable complexes with heavy metals.<sup>32</sup> Thus,

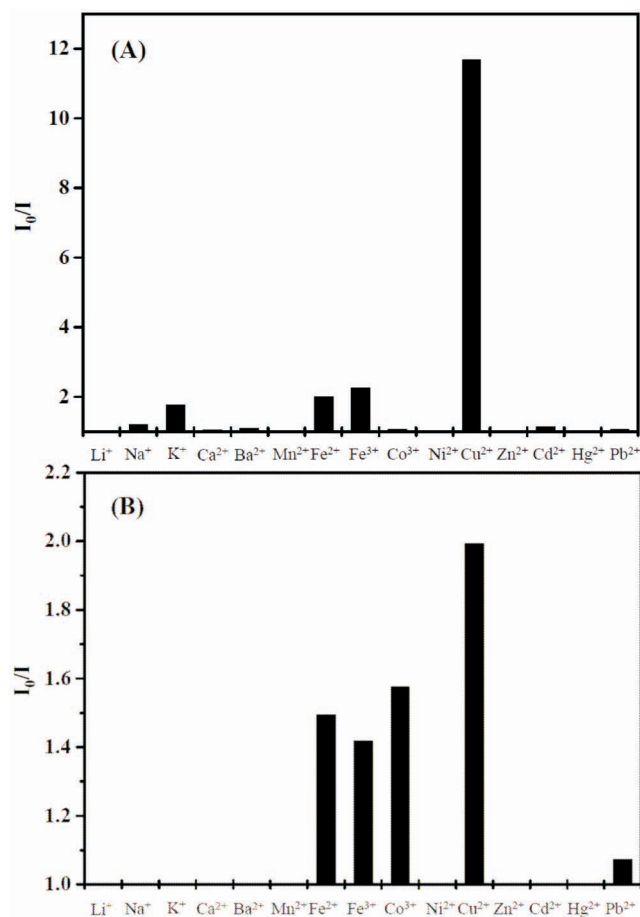


Fig. 3. The ratios ( $I_0/I$ ) of fluorescence intensity at 580 nm for (A) GSH-QDs and (B) PDDA/GSH-QDs composites upon the addition of 10  $\mu\text{M}$  metal ions.  $I_0$  and  $I$  denote the fluorescence intensities of (A) GSH-QDs and (B) PDDA/GSH-QDs in the absence and presence of metal ions. Buffer: 100 mM glycine at pH 7.0. The incubation time is 40 min. The excitation wavelength was set at 488 nm.

metal ion-induced fluorescence quenching of PDDA/GSH-QDs composites decreased with an increase in the concentration of glycine. Meanwhile, it is expected that the concentration of CuSe in PDDA/GSH-QDs composites was also diminished. To support our hypothesis, ICP-MS was used to determine the concentration of  $\text{Cu}^{2+}$  in the precipitates and supernatant after centrifugation of a mixture of PDDA/GSH-QDs composites, 10  $\mu\text{M}$   $\text{Cu}^{2+}$ , and 200–800 mM glycine. As expected, while the concentrations of glycine were changed from 200 to 800 mM, the concentrations of  $\text{Cu}^{2+}$  in precipitates (i.e. PDDA/GSH-QDs) and

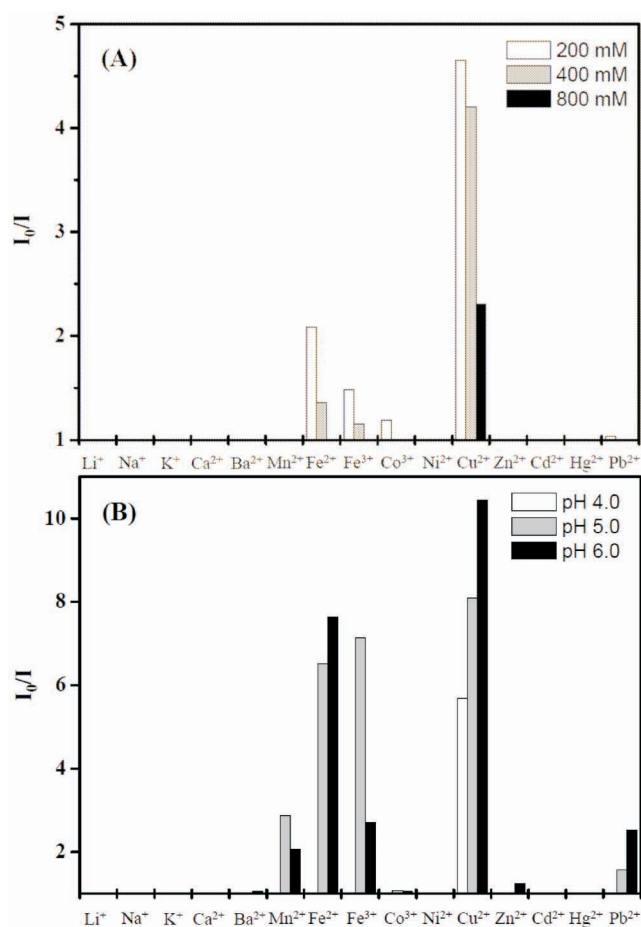


Fig. 4. Effect of (A) glycine concentration and (B) solution pH on the ratios ( $I_0/I$ ) of fluorescence intensity (580 nm) of PDDA/GSH-QDs composites upon the addition of 10  $\mu\text{M}$  metal ions. (A) PDDA/GSH-QDs composites were prepared in 200–800 mM glycine at pH 7.0. (B) PDDA/GSH-QDs composites were prepared in 800 mM glycine at pH 4.0–6.0. (A, B) The incubation time is 40 min. The excitation wavelength was set at 488 nm.



supernatants decreased from 0.074 to 0.010 and from 0.046 to 0.096 ppm, respectively. Additionally, the effect of solution pH on the selectivity of PDDA/GSH-QDs composites toward  $\text{Cu}^{2+}$  was investigated by comparing the ratio of fluorescence intensity ( $I_0/I$ ). As indicated in Fig. 4B, in 800 mM glycine solution at pH 4.0, the selectivity of this probe toward  $\text{Cu}^{2+}$  is apparently high over other metal ions. In contrast, the interferences of  $\text{Fe}^{2+}$ ,  $\text{Fe}^{3+}$ ,  $\text{Co}^{2+}$ , and  $\text{Pb}^{2+}$  for this probe were still existed in the case of both pH 5.0 and 6.0. It is probably because the formation constant of metal-glycine complex is highly dependent of solution pH.<sup>33</sup> Based on these results, we conclude that modification of GSH-QDs with PDDA, solution pH, and the concentration of glycine are essential parts of improving the selectivity toward  $\text{Cu}^{2+}$ .

#### Sensitivity of PDDA/GSH-QDs Composites

The fluorescence quenching reached completion within 1 h, the time frame of these measurements; thus, the reaction time was fixed at 1 h in quantitative analysis. Fig. 5A displays that the intensity of the fluorescence emission of PDDA/GSH-QDs composites was susceptible to  $\text{Cu}^{2+}$  and decreased as the concentration of  $\text{Cu}^{2+}$  increased. Three calibration curve were constructed by a linear regress of the logarithm of the fluorescence intensity ratio ( $I_0/I$ ) against the logarithm of the  $\text{Cu}^{2+}$  concentration (Inset a, b and c in Fig. 5B). The correlation coefficient ( $R^2$ ) were 0.990, 0.990, and 0.991 for the determination of  $\text{Cu}^{2+}$  in the range of  $3 \times 10^{-5} - 1 \times 10^{-4}$ ,  $1 \times 10^{-7} - 1 \times 10^{-5}$ , and  $1 \times 10^{-7} - 6 \times 10^{-10}$  M, respectively. The limit of detection (LOD) at a signal to noise ( $S/N$ ) ratio of 3 for  $\text{Cu}^{2+}$  was 0.2 nM ( $\sim 2.0$  ppt); the lowest detection concentration of  $\text{Cu}^{2+}$  was 0.6 nM ( $\sim 3.8$  ppt). In contrast to QD-based probes for the sensing of  $\text{Cu}^{2+}$ , the PDDA/GSH-QDs composites provided sensitivity improvement of about 1-3 orders of magnitude (Table 1).

## EXPERIMENTAL SECTION

### Chemicals

PDDAC (M. W. 400,000–500,000, 20 wt. % in water), glutathione, sodium borohydride, Rhodamine 6G, selenium powder, methanol, glycine, metallic salts, NaOH and HCl were all purchased from Aldrich (Milwaukee, WI). The pH values of glycine solution were adjusted by adding NaOH or HCl. All metallic salts were dissolved in deionized water. Milli-Q ultrapure water was used in all of the experiments.

### Characterization of GSH-QDs and PDDA/GSH-QDs Composites

A Hitachi F-4500 fluorometer (Hitachi, Tokyo, Japan) was used to measure the fluorescence spectra of QDs while the excitation wavelength was set at 488 nm. The average sizes of GSH-QDs and PDDA/GSH-QDs composites were determined by conducting transmission electron mi-

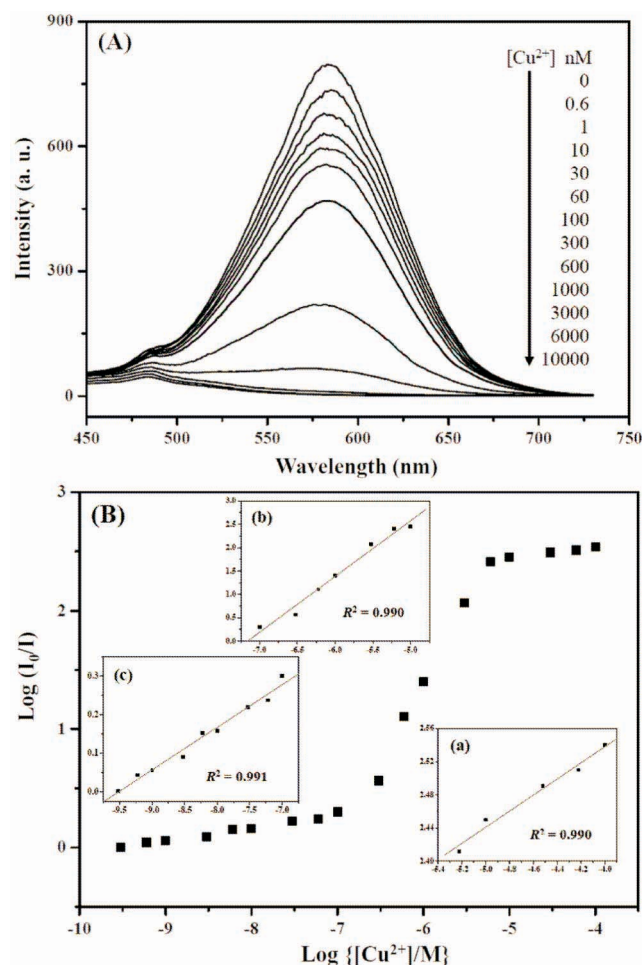


Fig. 5. (A) Fluorescence response of PDDA/GSH-QDs composites upon the addition of  $\text{Cu}^{2+}$  (0.6, 1, 10, 30, 60, 100, 300, 600, 1000, 3000, and 6000 nM). Inset: Time course measurement of the fluorescence intensity (580 nm) for PDDA/GSH-QDs composites upon the addition of 10  $\mu\text{M}$   $\text{Cu}^{2+}$ . (B) The logarithm of the fluorescence intensity ratio ( $I_0/I$ ) of PDDA/GSH-QDs composites versus the logarithm of the  $\text{Cu}^{2+}$  concentration. Inset: A calibration curve was obtained for the concentration range of (a)  $3 \times 10^{-5} - 1 \times 10^{-4}$ , (b)  $1 \times 10^{-7} - 1 \times 10^{-5}$ , and (c)  $1 \times 10^{-7} - 6 \times 10^{-10}$  M. Buffer: 800 mM glycine at pH 4.0. The incubation time is 60 min. The excitation wavelength was set at 488 nm.

Table 1. A comparison of PDDA/GSH-QDs composites and other sensors for the detection of  $\text{Cu}^{2+}$ 

Sensor <sup>a</sup>	Selectivity	Detection	LOD (nM)	Ref.
QIQET-modified silicon nanowire	$\text{Cu}^{2+}$ , $\text{Zn}^{2+}$	Fluorescence quenching	10	[14]
Spiropyran derivative	$\text{Cu}^{2+}$	Fluorescence inner filter effect	150	[15]
Zinc porphyrin-dipyridylamino	$\text{Cu}^{2+}$	Fluorescence quenching	330	[16]
Fluorophore-DNA conjugates	$\text{Cu}^{2+}$ , $\text{Co}^{2+}$ , $\text{Ni}^{2+}$	Fluorescence resonance energy transfer	20	[17]
DPPCA-modified gold nanoparticles	$\text{Cu}^{2+}$ , $\text{Co}^{2+}$ , $\text{Fe}^{3+}$ , $\text{Ni}^{2+}$ , $\text{Zn}^{2+}$ , $\text{Pb}^{2+}$	Fluorescence resonance energy transfer	1000	[18]
DNAzyme catalytic beacons	$\text{Cu}^{2+}$	Fluorescence resonance energy transfer	35	[19]
BSA-capped CdSe-ZnSe	$\text{Cu}^{2+}$ , $\text{Fe}^{3+}$	Fluorescence quenching	10	[20]
Peptide-capped CdS	$\text{Cu}^{2+}$ , $\text{Ag}^{+}$	Fluorescence quenching	500	[21]
Thioglycerol-capped CdS	$\text{Cu}^{2+}$ , $\text{Fe}^{3+}$	Fluorescence quenching	100	[22]
MSA-capped CdSe	$\text{Cu}^{2+}$	Fluorescence quenching	3.2	[23]
MPA-capped CdTe	$\text{Cu}^{2+}$ , $\text{Hg}^{2+}$ , $\text{Al}^{3+}$	Fluorescence quenching	3.0	[24]
CdTe nanowires	$\text{Cu}^{2+}$	Fluorescence quenching	78	[25]
PDDA/GSH-QDs	$\text{Cu}^{2+}$	Fluorescence quenching	0.2	This study

<sup>a</sup> QIQET: *N*-(quinoline-8-yl)-2-(3-triethoxysilyl-propylamino)-acetamide; DPPCA: *N,N*-2,6-diisopropylphenyl-1,7-dibromoperylene-3,4,9,10-tetracarboxylic acid bisimide; MSA: 2-mercaptoethane sulfonic acid; MPA: 3-mercaptopropionic acid.

croscopy (TEM) measurements (TEM, Tecnai G2 F20 S-Twin) and dynamic light scattering (DLS) using a N5 Submicron Particle Size Analyzer (Beckman Coulter Inc., USA). The dark-field images of GSH-QDs and PDDA/GSH-QDs composites were examined by homemade dark-field microscope (DFM), which consisted of an Olympus IX71 inverted microscope (Tokyo, Japan), an objective (40 $\times$ ; numerical apertures = 0.75), a digital camera (DP70, Olympus, Tokyo, Japan), a 100-W halogen lamp, and a condenser (IX-ULWCD, Olympus, Japan).<sup>27</sup> The quantum yields of the QDs were estimated by using Rhodamine 6G as a reference standard (Rhodamine 6G solution were prepared in ethanol, quantum yields = 95%).<sup>28</sup> The fluorescent images of the QD solutions were recorded using a Coolpix 5400 digital color camera (Nikon, Tokyo, Japan) while they were illuminated (365 nm) using a UVGL-25 UV lamp (Upland, CA, USA). The composition of QDs was determined by ELAN 6100 DRC ICP-MS (Perkin Elmer-SCIEX, Thornhill, ON, Canada) after the excess  $\text{Zn}^{2+}$ ,  $\text{Hg}^{2+}$ , NaHSe, and GSH were removed and then digested in a standard HCl/HNO<sub>3</sub> solution.

#### Synthesis of GSH-capped ZnHgSe QDs

Sodium borohydride (0.08 g) was reacted with selenium powder (0.079 g) in water (1.0 mL) to produce sodium hydrogen selenium (NaHSe, 0.99 M). The fresh NaHSe solution (20  $\mu\text{L}$ ) was then added to a N<sub>2</sub>-saturated mixture (15 mL) of Zn(ClO<sub>4</sub>)<sub>2</sub> (0.1 M; 700  $\mu\text{L}$ ), Hg(ClO<sub>4</sub>)<sub>2</sub> (0.1 M; 20  $\mu\text{L}$ ), and GSH stabilizer (0.05 M; 3.5 mL). The pH of the resulting mixture was adjusted to 7.0 by adding 1

M NaOH. The molar ratios of  $\text{Zn}^{2+}$ : $\text{Hg}^{2+}$  used in our experiment was 35:1. The resulting mixture was reacted at 95 °C within 60 min and resulted in the formation of Zn<sub>0.96</sub>Hg<sub>0.04</sub>Se QDs. The quantum yields and particle size of Zn<sub>0.96</sub>Hg<sub>0.04</sub>Se QDs are 78% and 4.5 nm, respectively (data not shown). No aggregation and no significant changes in their spectral characteristics were detected during several months in the dark.

#### Preparation of PDDA/GSH-QDs Composites

15 mL of GSH-QDs were concentrated to 5 mL by rotary evaporation. After that, 15 mL of methanol was added to a concentrated QD solution, resulting in precipitation of QDs. The resulting solution were subjected to two centrifuge-wash cycles to remove the excess  $\text{Zn}^{2+}$ ,  $\text{Hg}^{2+}$ , NaHSe, and GSH that were physically adsorbed onto the surface of GSH-QDs; centrifugation was conducted at 3000 rpm for 10 min and methanol was used for washing in each cycle. The precipitates were redissolved in 2 mL of water. Prior to the analysis of metal ions, 20  $\mu\text{L}$  of as-prepared GSH-QDs was blended with 100  $\mu\text{L}$  of 1.6% PDDAC. A homogeneous solution of PDDA/GSH-QDs composites was obtained by ultrasonication for 10 min.

#### Sample preparation

A solution of GSH-QDs or PDDA/GSH-QDs composites (120  $\mu\text{L}$ ) was added to 880  $\mu\text{L}$  of metal ions, which were prepared in 10-910 mM glycine solution with pH ranges of 4.0-7.0. The resulting mixtures were maintained in the dark at room temperature for 40 min and then transferred separately into a 1-mL quartz cuvette. Their fluores-

cent spectra were obtained using fluorescence spectrophotometer operated at an excitation wavelength at 488 nm.

## CONCLUSIONS

We have demonstrated a highly selective and sensitive approach for detection of  $\text{Cu}^{2+}$  based on the fluorescence quenching of PDDA/GSH-QDs composites. As compared to GSH-QDs, the selectivity toward  $\text{Cu}^{2+}$  was improved by modifying GSH-QDs with PDDA. Moreover, the selectivity of PDDA/GSH-QDs composites toward  $\text{Cu}^{2+}$  was apparently high by increasing glycine concentration and decreasing solution pH. The present approach offers the advantages of simplicity, high sensitivity, and high selectivity over the conventional methods (Table 1). It is believed that the proposed method may serve as a foundation for the preparation of practical sensors for the rapid determination of  $\text{Cu}^{2+}$  concentrations in aqueous environmental and biological samples.

## ACKNOWLEDGMENT

We would like to thank National Science Council (NSC 98-2113-M-110-009-MY3) and National Sun Yat-sen University and Center for Nanoscience & Nanotechnology.

## REFERENCES

1. Lynes, M. A.; Kang, Y. J.; Sensi, S. L.; Perdrizet, G. A.; Hightower, L. E. *Ann. N. Y. Acad. Sci.* **2007**, *1113*, 159-72.
2. Flemming, C. A.; Trevors, J. T. *Water, Air, Soil Pollut.* **1989**, *44*, 143-158.
3. Tapiero, H.; Townsend, D. M.; Tew, K. D. *Biomed. Pharmacother.* **2003**, *57*, 386-398.
4. Georgopoulos, P. G.; Roy, A.; Yonone-Lioy, M. J.; Opiekun, R. E.; Lioy, P. J. *J. Toxicol. Environ. Health, Part B* **2001**, *4*, 341-394.
5. (a) Waggoner, D. J.; Bartnikas, T. B.; Gitlin, J. D. *Neurobiol. Disease* **1999**, *6*, 221-230. (b) Bull, P. C.; Thomas, G. R.; Rommens, J. M.; Forbes, J. R.; Cox, D. W. *Nat. Genet.* **1993**, *5*, 327-337.
6. Barnham, K. J.; Masters, C. L.; Bush, A. I. *Nat. Rev. Drug Discovery* **2004**, *3*, 205-214.
7. Bruijn, L. I.; Miller, T. M.; Cleveland, D. W. *Annu. Rev. Neurosci.* **2004**, *27*, 723-749.
8. Brown, D. R.; Kozlowski, H. *Dalton Trans.* **2004**, 1907-1917.
9. United States Environmental Protection Agency Consumer Fact Sheet on Copper, 2011. [www.epa.gov/drink/contaminants/basic-information/copper.stm](http://www.epa.gov/drink/contaminants/basic-information/copper.stm) (Accessed April 20, 2011)
10. Xie, F.; Lin, X.; Wu, X.; Xie, Z. *Talanta* **2008**, *74*, 836-843.
11. Wu, J.; Boyle, E. A. *Anal. Chem.* **1997**, *69*, 2464-2470.
12. Liu, A.-C.; Chen, D.-c.; Lin, C.-C.; Cjou, H.-H.; Chen, C.-H. *Anal. Chem.* **1999**, *71*, 1549-1552.
13. Shervedani, R. K.; Mozaffari, S. A. *Anal. Chem.* **2006**, *78*, 4957-4963.
14. Mu, L.; Shi, W.; Chang, J. C.; Lee, S.-T. *Nano Lett.* **2008**, *8*, 104-109.
15. Shao, N.; Zhang, Y.; Cheung, S.; Yang, R.; Chan, W.; Mo, T.; Li, K.; Liu, F. *Anal. Chem.* **2005**, *77*, 7294-7303.
16. Weng, Y.-Q.; Yue, F.; Zhong, Y.-R.; Ye, B.-H. *Inorg. Chem.* **2007**, *46*, 7749-7755.
17. Mokhir, A.; Kiel, A.; Herten, D.-P.; Kraemer, R. *Inorg. Chem.* **2005**, *44*, 5661-5666.
18. He, X.; Liu, H.; Li, Y.; Wang, S.; Li, Y.; Wang, N.; Xiao, J.; Xu, X.; Zhu, D. *Adv. Mater.* **2005**, *17*, 2811-2815.
19. Liu, J.; Lu, Y. *J. Am. Chem. Soc.* **2007**, *129*, 9838-9839.
20. Xie, H. Y.; Liang, J. G.; Zhang, Z. L.; Liu, Y.; He, Z. K.; Pan, D. W. *Spectrochim. Acta, Part A* **2004**, *60*, 2527-2530.
21. Gattás-Asfura, K. M.; Leblanc, R. M. *Chem. Commun.* **2003**, 2684-2685.
22. Chen, Y.; Rosenzweig, Z. *Anal. Chem.* **2002**, *74*, 5132-5138.
23. Fernandez-Arguelles, M. T.; Wei, J. J.; Costa-Fernandez, J. M.; Pereiro, R. Sanz-Medel, A. *Anal. Chim. Acta*, **2005**, *549*, 20-25.
24. Bo, C.; Ping, Z. *Anal. Bioanal. Chem.* **2005**, *381*, 986-992.
25. Tang, B.; Niu, J.; Yu, C.; Zhuo, L.; Ge, J. *Chem. Commun.* **2005**, 4184-4186.
26. Liu, F.-C.; Tseng, W.-L.; Cheng, T.-L.; Shen, C.-C.; Chiang, M. Y. *Langmuir* **2008**, *24*, 2162-2167.
27. Tseng, W.-L.; Lee, K.-H.; Chang, H.-T. *Langmuir* **2005**, *21*, 10676-10683.
28. Tonti, D.; van Mourik, F.; Chergui, M. *Nano Lett.* **2004**, *4*, 2483-2487.
29. Isarov, A. V.; Chrysochoos, J. *Langmuir* **1997**, *13*, 3142-3149.
30. Chen, J.; Zheng, A.; Gao, Y.; He, C.; Wu, G.; Chen, Y.; Kai, X.; Zhu, C. *Spectrochim. Acta, Part A* **2008**, *69*, 1044-1052.
31. Mansson, S.; Colleen, S.; Mardh, P.-A. *Eur. Urol.* **1989**, *16*, 18-22.
32. (a) Marino, T.; Toscano, M.; Russo, N.; Grand, A. *J. Phys. Chem. B* **2006**, *110*, 24666-24673. (b) Remko, M.; Rode, B. M. *J. Phys. Chem. A* **2006**, *110*, 1960-1967.
33. Fan, J. Shen, X.; Wang, J. *Electroanalysis* **2001**, *13*, 1115-1118.